Atmos. Chem. Phys. Discuss., 8, 7509–7554, 2008
www.atmos-chem-phys-discuss.net/8/7509/2008/

Atmospheric Chemistry and Physics Discussions

Lagrangian analysis of low level anthropogenic plume processing across the North Atlantic

E. Real[1,*], K. Law[1], H. Schlager[2], A. Roiger[2], H. Huntrieser[2], J. Methven[3], M. Cain[3], J. Holloway[4], J. A. Neuman[4], T. Ryerson[5], F. Flocke[6], J. de Gouw[4], E. Atlas[7], S. Donnelly[8], and D. Parrish[5]

[1]Service d'Aéronomie, 3ème étage, Tour 45-46, 4 Place Jussieu, 75005 Paris, France
[2]Deutsches Zentrum für Luft- und Raumfahrt (DLR), Oberpfaffenhofen, Institut für Physik der Atmosphäre, 82230 Wessling, Germany
[3]Departement of Meteorology, University of Reading, PO Box 243, Earley Gate, Reading, RG6 6BB, UK
[4] NOAA ESRL / CIRES, University of Colorado at Boulder, Boulder CO 80309, USA
[5]NOAA ESRL, 325 Brodway, Boulder, CO 80305, USA
[6]Atmospheric Chemistry Division, NCAR, 1850 Table Mesa Drive Boulder, CO 80305, USA
[7]RSMAS/MAC University of Miami, Miami, FL 33149 USA
[8]Departement of Chemistry, Fort Hays State University, Hays KS 67601, USA
[*]now at: CEREA, a Joint Laboratory ENPC/EDF R&D, 6–8 avenue Blaise Pascal, Cité Descartes Champs-sur-Marne, 77455 Marne la Vallée, France

Received: 12 March 2008 – Accepted: 26 March 2008 – Published: 17 April 2008

Correspondence to: E. Real (elsa.real@aero.jussieu.fr)

Published by Copernicus Publications on behalf of the European Geosciences Union.

Abstract

The photochemical evolution of an anthropogenic plume from the New-York/Boston region during its transport at low altitudes over the North Atlantic to the European west coast has been studied using a Lagrangian framework. This plume, originally strongly polluted, was sampled by research aircraft just off the North American east coast on 3 successive days, and 3 days downwind off the west coast of Ireland where another aircraft re-sampled a weakly polluted plume. Changes in trace gas concentrations during transport were reproduced using a photochemical trajectory model including deposition and mixing effects. Chemical and wet deposition processing dominated the evolution of all pollutants in the plume. The mean net O_3 production was evaluated to be -5 ppbv/day leading to low values of O_3 by the time the plume reached Europe. Wet deposition of nitric acid was responsible for an 80% reduction in this O_3 production. If the plume had not encountered precipitation, it would have reached the Europe with O_3 levels up to 80-90 ppbv, and CO levels between 120 and 140 ppbv. Photochemical destruction also played a more important role than mixing in the evolution of plume CO due to high levels of both O_3 and water vapour showing that CO cannot always be used as a tracer for polluted air masses, especially for plumes transported at low altitudes. The results also show that, in this case, an important increase in the O_3/CO slope can be attributed to chemical destruction of CO and not to photochemical O_3 production as is often assumed.

1 Introduction

It is recognised that emissions from large urban/industrial regions can have large-scale impacts on levels of O_3, particles, and other trace constituents downwind from continents. These impacts are important because they may affect the ability of downwind countries to meet air quality standards, and because of the climate impacts of O_3 and particles through radiative forcing. Anthropogenic pollution occurs primarily in the

ACPD

8, 7509–7554, 2008

boundary layer (BL) over continents. This pollution may then be transported at low levels directly impacting the BL of a downwind continent or may be exported from the BL into the mid and upper troposphere by frontal systems or convection and transported at higher altitudes (Li et al., 2005). Because of lower water vapour and temperature, loss processes are less active and pollutant lifetimes are longer in the upper troposphere. However, high altitude plumes are less likely to directly impact the BL composition of a downwind continent. Several modelling studies have already shown that long-range transport of pollutants from North America to Europe is one of the most important due to large emissions and relative proximity of the two continents (Wild and Akimoto, 2001; Stohl, 2001; Stohl et al., 2002). There is clear experimental and modelling evidence for such export from North America at both low and high altitudes. Polluted plumes have been sampled at remote surface sites such as Sable Island or Chebogue Point (Parrish et al., 1998; Millet et al., 2006), off the New England coast, and also downwind in the Azores (Parrish et al., 1998; Owen et al., 2006) in the mid Atlantic Ocean. Analysis of these polluted plumes showed that they were usually transported at low altitudes, below 3 km. Modelling studies suggest that one third of CO exported from North America occurs in the lowest 3 km (Li et al., 2005) and Owen et al. (2006) suggested that low level transport of North American pollution above the marine BL may provide an effective mechanism for long-range transport of anthropogenic pollution over the Atlantic ocean with a resulting impact on lower tropospheric O_3 in downwind regions.

Whilst there have been several measurements of polluted plumes with North American origins in the free troposphere over Europe (e.g. Huntrieser et al., 2005), there have been fewer detailed cases at low levels and the impact of such long-range transport on O_3 levels in the European BL is not well documented (Derwent et al., 1998). Ground-based sites on the west coast of Europe do occasionally observe such cases. For example, Li et al. (2002) reported several measurements of moderately polluted plumes at Mace Head (west coast of Ireland) with weak enhancements in CO and O_3. Despite the relative lack of experimental evidence, global model simulations suggest that the impact of anthropogenic North American pollution on European BL O_3 is im-

portant. Li et al. (2002) and Auvray and Bey (2005) estimated an increase of 2 to 4 parts per billion by volume (ppbv) in European O_3 concentrations during summer, which could be responsible for 20% of the violation of the European Union threshold for O_3. These studies suggest that half of the import of North American O_3 in the BL is due to transport at low altitudes with the remainder due to subsidence of high altitude plumes. Derwent et al. (2004) suggested a higher value of 8 ppbv increase in the European BL using an O_3 tracer technique in a semi-Lagrangian global model. During high pollution events, under conditions typified by a strong Icelandic Low located between Iceland and the British Isles, Auvray and Bey (2005) simulated an increase of European O_3 due to North American pollution of more than than 10 ppbv. Several explanations have been proposed for the difference between the non-negligible impact of North American pollution on Europeean O_3 simulated by models and the lack of experimental evidence. Stohl et al. (2002) suggested that North American pollution reaches the European BL primarily south of the Pyrenees where measurement sites are sparse, and also that North American plumes are generally older then 10 days when reaching Europe, and therefore, hard to accurately trace back to sources.

In this study we address these issues through the analysis of data collected in a pollution plume transported at low level over the North Atlantic as part of the International Consortium for Atmospheric Research on Transport and Transformation (ICARTT) (Fehsenfeld et al., 2006) also encompassing the European Intercontinental Transport of Ozone and Precusors (ITOP) experiment, which took place in summer 2004. As part of this campaign, the International Transport and Chemical Transformation (ITCT)- Lagrangian 2K4-experiment (an IGAC task) executed a Lagrangian study of polluted air masses transported across the North Atlantic. Four research aircraft based in North America, the Azores and western Europe sampled the same air masses several times during long-range transport. Lagrangian experiments have been conducted previously, but this was the first time that a Lagrangian experiment was conducted in the free troposphere on intercontinental scales. The main advantage of this kind of study is that changes in a plume concentrations over several days can be estimated by compar-

ing two Lagrangian samplings, and the processes leading to these changes can be evaluated with reduced uncertainty. After the campaign a detailed analysis using trajectories, a Lagrangian dispersion model, and in-situ measurements was performed by Methven et al. (2006), and showed that there were five cases where the same air mass had been sampled several time across the Atlantic.

The overall goal of this paper is to improve our understanding about low level long-range transport of anthropogenic plumes over the North Atlantic and their impact on O_3 and precursors levels over Europe. In particular, we analyse the evolution of a North American plume observed during the Lagrangian 2K4 experiment which was originally very polluted, and then transported at low levels over the North Atlantic toward Europe. The aim is also to determine the relative importance of processes influencing its chemical composition, and to explain why polluted North American plumes are not easily detected at surface measurement sites over Europe.

The Lagrangian plume in question originated from the New York-Boston conurbation and was sampled 3 times just off the New England coast on 3 successive days by the National Oceanic and Atmospheric Administration (NOAA) P3, and then, 2 days later off the west coast of Ireland, and 3 days later over the English Channel by the German Deutsches Zentrum fur Luft- und Raumfahrt (DLR) Falcon. First, the Lagrangian matches identified by Methven et al. (2006) are discussed in Sect. 2 together with the observed chemical evolution of pollutants during the plume transport. Cases where the Lagrangian matching is less good due to the influence of other processes such as mixing with local emissions are also identified. Next, to evaluate the relative contributions of chemical, physical and dynamical processes to changes in O_3 concentrations in the plume during transport, a photochemical trajectory model was used (Sect. 3). In Sect. 4, results are presented from model runs initialised with upwind data over New England, and compared to downwind data over Europe. The model was run along a trajectory representative of the mean plume transport pathway and giving the best match between plume samplings. The model was first run with chemistry only (Sect. 4.1), and then including wet and dry deposition (Sect. 4.2) as well as mixing with air masses in

close proximity to the plume (Sect. 4.3). The ability of the model to simulate the contribution of photochemical processes to O_3 changes in the plume was further tested by examining the evolution of trace gas correlations using multiple model runs initialised across the first plume sampling (Sect. 4.4). Conclusions are presented in Sect. 5.

2 Lagrangian case: measurements and analysis

2.1 Identification of Lagrangian matches

Methven et al. (2006) used a novel technique to identify Lagrangian matches between flight segments from different aircraft during the entire IGAC Lagrangian 2K4 campaign in July 2004. This technique combined trajectories, calculated using global meteorological analysis (European Center for Medium Range Weather Forecast 40 year Reanalysis; ERA-40), and hydrocarbon fingerprint analysis. A match was defined as an occasion when a pair of whole air samples (analysed for their hydrocarbon content) collected during different flights exhibited highly correlated hydrocarbon fingerprints (when such measurements were available), and the sample time windows were also connected by both backward and forward trajectories. Results from the Lagrangian particle dispersion model, FLEXPART, run with CO tracers (Stohl et al., 2004) were also used to confirm matches. Five clear Lagrangian cases covering a variety of situations were identified. Further details can be found in Methven et al. (2006).

In this paper, we build on the work of Real et al. (2007) which focused on the Lagrangian analysis of the forest fire case, also discussed by Methven et al. (2006), with the examination of the case of low level pollutant plume transport. An anthropogenic plume from New York-Boston was sampled first by the NOAA P3 over the Gulf of Maine and Nova Scotia on 3 successive days (20, 21, 22 July), and then by the DLR Falcon flying just off the coast of Ireland on 25 July and over the English Channel on 26 July 2004. The flight tracks of these 5 flights are shown in Fig. 1. The segments of the 3 flights identified as Lagrangian matches were labelled as Lagrangian case 3 by

Methven et al. (2006). The same Lagrangian time windows are used in this study. The ability of the Methven et al. (2006) analysis to identify Lagrangian matches has been shown to work well in the free troposphere where transport is mainly driven by advection (Real et al., 2007). However at low altitudes, certain meteorological features are not well resolved by analysed winds, and can induce errors in the Lagrangian analysis. For example, Riddle et al. (2006) analysed the ability of trajectory models to represent air mass transport during the ICARTT campaign by using Lagrangian balloons. These balloons were launched close to the Lagrangian match of the NOAA-P3 aircraft on 20 July. On 21 July, the balloon location and aircraft Lagrangian match were very well co-located (less than 2 km apart) suggesting that the matching between these 2 samples is good. However, this is not the case for 22 July. Important differences were found between balloon and model trajectories between 21 and 22 July over the Newfoundland coast, maybe due to poor simulation of strong coastal winds in the ECMWF analyses. Moreover, the hydrocarbon match on 22 July was the least consistent. Therefore, it appears that Lagrangian match on 22 July is less good. The accuracy of the Lagrangian samplings is discussed further in the next section where the observations in the plume segments are discussed.

The meteorological situation during plume transport has been examined using the Geodetic Earth Orbiting Satellite GOES-1 and METEOSAT satellite images superimposed with surface pressure values (see Fig. 3). On 19 July, a cold front passed over the north-east coast of the United States (US). Behind this front, strong outflow took place below 3 km transporting air from the New York-Boston region on 20 July towards Newfoundland on 22 July. From the 22 to 25 July, strong winds established over the Atlantic Ocean between the Azores/Bermuda High and the Icelandic Low, particularly on 22 July, which transported the polluted plume to Europe. On 25 July the Icelandic Low moved northward allowing the air masses to reach the Irish coast. This low level export from the North American east coast in conjunction with a cold front is a classical feature of North American summertime meteorology, and has been shown by, for example, Li et al. (2005) to be an important factor driving summertime pollution export. Warm con-

veyor belts associated with cold fronts lift pollution from the central and north-eastern US into the upper troposphere over Newfoundland, and strong north-eastward outflow takes places at low level behind the cold front. Li et al. (2005) evaluated the occurrence of such events to be 5 to 7 per month in summer. The transport over the North Atlantic towards Europe is then dependent on the Azores High/Icelandic Low position and strength. Guerova et al. (2006) reported that of the export events identified by Li et al. (2005), 3 reached central Europe, with about half at low levels. Li et al. (2002) evaluated a higher frequency of low level North American plumes reaching Europe during summer 1994 to 1997. The plume studied here is a case of this kind of pollutant export.

2.2 Chemical composition of the Lagrangian matches

Detailed information about the instrumentation on board the aircraft can be found in Fehsenfeld et al. (2006). Since measurements taken by the different aircraft will be used to infer the chemical evolution of the plume, it is important to compare these measurements. Several comparison flights were performed between the 4 aircrafts involved in the campaign. Overall, the comparison indicated that O_3 measurements agree within 2 ppbv and CO within 3 ppbv, for the aircraft used in this study. Comparison of hydrocarbons was more difficult but where possible, comparison showed good agreement. More details about the comparison flights can be found in Methven et al. (2006) and Fehsenfeld et al. (2006). The general behaviour of the plume evolution is first examined in terms of observed trace gas mean values and correlations. Observed concentrations of O_3, NO and NO_y with respect to CO in the 5 Lagrangian matches are shown in Fig. 2 with averaged values during the 5 match time windows reported in Table 1. Correlation coefficients, r, and slopes were also calculated and provide information about the dispersion of data around the correlation line, and therefore, the quality of the correlation. These results are given in Table 4 and are also discussed later in Sect. 4.4 when they are compared to model simulations.

The first interception of the plume by the P3 on 20 July showed a highly polluted

plume with high values of CO (200 ppbv) very well correlated (r=0.91) with high values of O_3 (90 ppbv), NO_x (500 pptv) and very high levels of NO_y (15 550 pptv). Here, NO_y was mainly in the form of HNO_3 representing approximately 92% of total NO_y. One day later, CO, O_3 and NO_x levels slightly decreased, but remained elevated. HNO_3 concentrations showed the strongest decrease to only 32% of the initial value. O_3 and CO were still highly correlated with a similar slope (0.51) whereas the slope between NO and CO decreased strongly even though the two species were still very well correlated (r=0.85). On 22 July, CO, NO_x, PAN, HNO_3 and O_3 levels decreased and the species are not correlated anymore with value of r between 0.14 and 0.3. Moreover, concentrations of the main volatile organic compounds (VOCs) (C_2H_6, C_2H_4, C_5H_8, CH_3OH, acetone) increased and are higher than on the first Lagrangian sampling. This lack of correlation as well as the increase in VOCs could be explained by very strong and inhomogeneous mixing with another air mass, or as previously discussed this match appears to be incorrect due to large uncertainties in the calculation of trajectories on this day. Therefore, although comparisons between model results and data on 22 July are shown, the uncertainty surronding this match should be kept in mind

The 3 North American interceptions (20, 21 and 22 July) were made close to remote surface sites in New England (Sable Island, Chebogue Point and Appledore Island). Polluted plumes from the New York-Boston region are often encountered in this region, as shown by Chen et al. (2007) who estimated that these events occurred 15% of the time during summer 2004. Comparison of measurements in the Lagrangian match and those analysed by Parrish et al. (1998) at Sable Island and Chebogue Point between 1991–1994, shows that the mean O_3 and CO values as well as the O_3/CO measured slopes are in the upper range of the surface observations. The aircraft observations were collected above the surface and were probably subject to less dry deposition of O_3. Another factor that can explain the larger O_3/CO slope is that the NO_x to CO emission ratio in the US has changed since the early 1990s. Assuming that the production of O_3 is NO_x limited, then steeper O_3/CO relationships could be expected in 2004 as suggested by Honrath et al. (2004).

After the plume crossed the North Atlantic it was intercepted on 25 July by the DLR Falcon aircraft off the west coast of Ireland. Lower concentrations of pollutants were measured with mean concentrations of 138 ppbv CO, 44 ppbv O_3, and 175 pptv NO_y, which represents only 2% of the initial NO_y value. Correlation between species are now very low including the O_3/CO slope (–0.03). Mean values and slopes can be compared with those measured in summer at Mace Head (53° N, 10° W), on the Irish west coast between 1994 to 1997 by Li et al. (2002). Indeed, using global model runs with and without North American sources, Li et al. (2002) estimated CO and O_3 levels in North American plumes reaching Mace Head. Mean values measured in the Lagrangian plume are typical of those evaluated by Li et al. (2002), but the O_3/CO slope is much less than the typical values of 0.2 to 0.4 reported by Li et al. (2002). Reasons for the discrepancies between these measured slopes are analysed further in Sect. 4.4. Although these O_3 value are much less than on the first sampling of the plume, they still represent an increase compared to background for the remote marine environment where the measurements were taken, i.e. 10 to 20 ppbv above average for O_3 and 10 to 40 ppbv for CO.

According to Methven et al. (2006), the plume was intercepted a last time by the Falcon over the English Channel on 26 July with CO and O_3 levels slightly lower than the previous day and a negative O_3/CO slope. As for NO and NO_y, measured levels strongly increased compared to the previous match and NO and NO_y levels were even higher than in the first match. This suggests that strong mixing with freshly polluted European air masses had taken place.

The evolution of the plume observed here seems fairly typical in terms of the reductions in pollutant levels during transport across the Atlantic and the transport pathway by cold front advection over the US followed by rapid transport towards Europe. Further analysis using a photochemical trajectory model and comparison with the observations in the Lagrangian match segments will provide an insight into the processes which are responsible for the observed plume evolution.

3 Modelling

The Lagrangian photochemical model, CiTTyCAT (CambrIdge Tropospheric TrajectorY model of Chemistry And Transport) has been used to examine the different processes influencing the evolution of trace gases within the plume, and in particular, O_3, CO and NO_y. CiTTyCAT has been used previsously to examine the origin of polluted layers over the North Atlantic during past campaigns (Wild et al., 1996; Evans et al., 2000). This model also successfully captured the trace gas evolution in the forest fire Lagrangian plume transported over the North Atlantic during ICARTT (Real et al., 2007) and identified by Methven et al. (2006). The model is considered as an isolated air parcel, and run along trajectories calculated using large-scale meteorological analyses. Ninety chemical species are treated in the model including degradation of 14 hydrocarbons using chemical rate data from JPL (2003), and updates discussed in Arnold et al. (2006). The photolysis scheme used in the runs presented here is based on a 2-stream multiple scattering scheme (Hough, 1988).

3.1 Chemical initialisation

The model was first used to try to reproduce the average evolution of average concentrations in the plume (Sects. 4.1, 4.2.1, 4.3). The model was initialised with concentrations measured in the plume on 20 July by the P3, and compared with average concentrations measured by the same aircraft on 21 and 22 July as well as by the Falcon on 25 and 26 July. These measured concentrations are indicated Table 1. The only species for which the initial value has not be taken from measurements is methane, with a typical value of 1.8 ppmv. In order to characterise the variability in plume concentrations, 3 simulations were carried out: one with mean concentrations measured during the plume match segment, and 2 others using the mean concentrations + (–) standard deviation (std). Note that all species are well correlated in the plume making this approach appropriate. Then, in order to extend the analysis the model was initialised across the full range of concentrations in each match segment

and their inter-relationships (correlations) analysed (Sect. 4.4).

3.2 Trajectories

The model was run along a trajectory calculated with the FLEXTRA model (Stohl et al., 1995) using ECMWF ERA-40 wind fields. Position, temperature and water vapour used in CiTTyCAT were interpolated from the FLEXTRA trajectory at every CiTTyCAT time-step. All trajectories initialised in the P3 Lagrangian match on 20 July showed approximately the same transport, so the one initialised around 21:20 was chosen (see Fig. 1). This trajectory passes closest to the P3 Lagrangian matches on 21 and 22 July, and the Falcon matches on 25 and 26 July.

3.3 Representation of physical phenomenon

Wet and dry deposition as well as mixing can be included in the model. Dry deposition is simulated when the air parcel is in the BL using a velocity parameter which depends on surface type and on the height of the BL. The BL was defined climatologically from GEOS-1 meteorological data (Schubert et al., 1993). The original wet deposition scheme is a simple scheme using a lifetime for soluble species. More details about the model can be found in Wild et al. (1996) and Evans et al. (2000). The model was first run with only photochemical processes (Sect. 4.1). in order to study the chemical evolution of the plume in absence of other processes. Then, since the plume was transported at low altitudes, and sometimes in the BL, runs were made including dry deposition (Sect. 4.2.1). GEOS METEOSAT satellite images (see Fig. 3) indicate the presence of clouds, on certain occasions in the same location as the plume, especially over the North American coast. Moreover, the strong decrease in HNO_3 measured in the plume is likely to be the result of wet deposition since HNO_3 is highly soluble. For this reason, runs were also carried out including wet deposition. In addition, a new scheme was implemented based on precipitation rates from ECMWF (Sect. 4.2.2). Note that aerosol levels in the plume were high initially but dropped between the 20

and 22 July from a number concentration of about $5.5\times10^3\,cm^{-3}$ to $3.0\times10^3\,cm^{-3}$, which may also indicate that deposition was active, even if other mechanisms (i.e. dilution, coagulation) can also explain this decrease. Heterogeneous reactions, were not included in the simulations discussed here. One of the main impacts of heterogeneous reactions is to through the conversion of NO_x into HNO_3 via the heterogeneous hydrolysis of N_2O_5 at night. This process may be important for NO_x budget but the rate for conversion (γ) is highly variable and may depend, in particular on the sulfate aerosol loading (Brown et al., 2006). Brown et al. (2006) evaluated a not negligible value of γ in the Newfoundland region during ICARTT, but less important than westward. It will be seen in Sect. 4.3 that NO_x levels in the plume are underestimated in the simulation, suggesting that the inclusion of heterogeneous N_2O_5 hydrolysis would not give better results in this case. Finally, mixing between the plume and surrounding air masses was also considered (Sect. 4.3).

4 Results

4.1 Chemistry-only simulations

Simulated concentrations of CO, O_3, NO, NO_2, HNO_3 and PAN for the model runs initialised with mean, mean +std and mean –std concentrations measured in the P3 Lagrangian match on 20 July are shown in Fig. 4 together with simulated O_3 production and destruction terms. Water vapour and temperature data interpolated along the trajectory from ECMWF analyses are also shown. These results include only changes due to chemical processes in the model.

4.1.1 Simulated plume characteristics

The modelled chemical evolution of the plume shows two interesting features. Firstly, despite high levels of water vapour, high concentrations of NO, NO_2, HNO_3 and O_3 are

maintained in the plume whereas PAN levels decrease rapidly due to high temperatures. Analysis of O_3 production and destruction terms shows that O_3 destruction due to water vapour is important, but is almost balanced by the O_3 production. Sensitivity tests will help to understand the origin of this high O_3 production (see Sect. 4.1.3). The second interesting feature is the high oxidising capacity of the plume. In these chemistry only simulations, OH levels remain high during the entire run with mean values of 4×10^6 molecs. cm^{-3} and peaks around 15×10^6 molecs. cm^{-3} around noon. This can be mainly explained by high water vapour, due to the low altitude of the plume, and high levels of O_3.

One of the main impacts of this high oxidising capacity is the strong photochemical destruction of CO, which decreases by about 50 ppbv in 6 days. CO is often considered as a pollution tracer, not really affected by chemical loss over a period of 10 days or less and a strong decrease in CO levels is usually attributed to dilution and mixing. In this case, assuming no other loss processes, CO levels decreased by 25% solely as a result of chemical destruction. This would imply that for this plume, transported at low altitudes, the CO chemical lifetime is about 20 days. This value can be compared with a value of 30 days for the global mean CO lifetime during summer.

4.1.2 Comparison of measured and simulated concentrations

The general evolution of measured PAN and CO values can be reproduced by chemical processing suggesting an important role for photochemistry in this case although CO is still overestimated after 6 days and PAN data were only available from the P3. Measured NO and NO_2 values are generally overestimated by the mean simulations, and are more represented by the mean –std simulation. O_3 values are overestimated by more than 40 ppbv after 5 days but the strongest difference is found between simulated and measured HNO_3 with average modelled concentrations 13 ppbv higher after 3 days. These differences suggest that other processes such as deposition and mixing were also important. Unfortunately, measurements of other species like H_2O_2 or HCHO for the three P3 flights were not available to provide further tests of the model

results discussed in the next sections. Concerning OH, simulated values are the same order of magnitude as those calculated by Warneke et al. (2004) using a box model initialised with measurements from a research ship along the New England coast, i.e. in the same region as the Lagrangian plume during the first 3 days, albeit at a lower altitude. However, the peak noon values simulated here are higher than those measured, for example, in the Los Angeles basin by George et al. (1999) (7×10^6 molecs.cm^{-3}), and by Ehhalt and Roher (2000) at a rural German site (12×10^6 molecs.cm^{-3}). Measured JO^1D and JNO_2 during the 3 first Lagrangian samplings are in good agreement with simulated values (not shown) but the model underestimates several VOCs: C_2H_2, C_2H_6, C_4H_10, C_2H_4 and C_3H_6 are underestimated by 70, 140, 20, 110 and 90 pptv respectively on the 25 July. Concerning water vapour and temperature, the difference between measured values and those interpolated from ECMWF analyses along the trajectory is always less than 20% for water vapour and 4K for temperature. Therefore, in these runs which only take chemical processes into account, the overestimation in O_3 is leading to an overestimation in OH and therefore other processes are also playing an important role as will be discussed in the following sections.

4.1.3 Sensitivity tests

In order to better understand photochemical processing in the plume and possible reasons for the differences between simulated and observed O_3, two sensitivity tests were performed. Firstly, initial HNO_3 concentrations were reduced to zero (S-noHNO_3) in order to study the role of HNO_3 in the net production of O_3 during transport. Secondly, a cloud with an optical depth of 5 (value of the mean cloud optical depth observed around the world by Rossow and Schiffer, 1991) was simulated just above the plume (S-CLOUD) in order to examine the maximum effect of a cloud layer on photolysis rates inside the plume. The S-CLOUD simulation is representative of a maximum effect because clouds were not present during the entire transport over the North Atlantic as shown by the GOES-METEOSAT satellite images. In particular, clouds were not present during the match periods when, as noted previously, modelled photolysis

rates agree well with the measurements. The chosen optical depth is also relatively high for non-convective clouds. In both cases simulations were initialised with mean values measured in the plume. Results of these sensitivity tests are shown in Fig. 5.

Results of the run S-noHNO_3 clearly show that the maintenance of high O_3 levels in the chemistry-only simulation is mainly due to HNO_3 photolysis. Indeed after 6 days, O_3 concentrations in the S-noHNO_3 simulation are lower than the reference simulation by about 35 ppbv, and the mean net O_3 production has decreased by 70%. One of the consequences of this is a reduction in the oxidising capacity of the plume (OH is reduced by 30%) leading to slightly higher simulated CO concentrations. It shows that when initial HNO_3 concentrations are high, the quantity of HNO_3 available for photolysis becomes non-negligible, and, in the absence of loss processes, HNO_3, which acts initially as a reservoir, then releases NO_2 during long-range transport. Neuman et al. (2006) also measured high HNO_3 in several other plumes during the ICARTT campaign, some of them as far as 1000 km downwind from source regions and showed the importance of HNO_3 in the production of O_3 in plumes rich in HNO_3. However, this strong role played by HNO_3 assumes a weak influence of wet deposition.

Concerning the S-CLOUD simulation, the presence of cloud above the plume is responsible for a reduction in photolysis rates (–9% for NO_2 rate and –7% for O_3 rate) in these runs. Since there are compensating effects both O_3 production and destruction are reduced and so the presence of cloud does not modify O_3 levels by much and cannot explain the difference in between observed and simulated O_3 values. Because of the O_3 photolysis reduction, the oxidising capacity of the plume is slightly reduced (by a few percent) and therefore CO destruction.

4.2 Chemistry and deposition simulations

4.2.1 Dry deposition

Results of model runs including photochemistry plus dry deposition are shown in Fig. 6 (orange lines). Dry deposition is simulated in the model when the plume is in the BL,

i.e. about 15% of the time. The BL definition in the model is climatologically defined, and so, not specifically calculated for the days of the study. The modelled BL heights for the Lagrangian matches were checked by plotting vertical profiles of water vapour observed by the P3 aircraft around the Lagrangian matches. In the BL, air masses are mixed and the water vapour profile should be relatively homogeneous whereas outside the BL it should exhibit strong vertical gradients. The profiles in Fig. 7 show that every time the aircraft was over ocean (profiles a) and part of profile b), the BL height was less than 0.4 km and so the plume was above it, whereas over land, it was between 1 and 1.5 km and the plume was in the BL. This corresponds well to the model simulation with no dry deposition simulated for the 2 first Lagrangian sampling (over sea) whereas dry deposition is active on 22 July (over land). Inclusion of dry deposition in the simulations leads to decreases of 8 and 20% in O_3 and HNO_3, respectively. However, it is clear that dry deposition alone cannot explain the observed decrease in either HNO_3 or O_3 in this plume. For a plume travelling at lower altitude and spending more time in the BL, a much more important impact of dry deposition could be expected. The results are also sensitive to the definition of the BL height and to positional errors in the trajectories as already discussed for 22 July in Sect. 2.

4.2.2 Wet deposition

As noted already, satellite images and the strong decrease of HNO_3 levels in the plume suggest that wet deposition was active during the transport of this plume away from source regions. In the basic model, wet deposition is parameterised using a local constant loss rate, r (s-1) (run S-WET1). In this study, two new schemes have also been implemented linking wet deposition to more realistic precipitation using column integrated precipitation rates, p (mm s^{-1}) calculated from ECMWF. The first scheme (S-WET2) is based on Walton et al. (1988) who introduced a wet deposition coefficient, S, such that $r = S \times p$. For a very soluble gas, such as HNO_3, Penner et al. (1991) suggested values of S equal to 2.4 mm^{-1} for stratiform precipitation, and 4.7 mm^{-1} for convective precipitation. The second scheme (S-WET3) uses a classical formula

for the simulation of wet loss of a very soluble species, $r=p/L$ were L represents the quantity of condensed water integrated over the tropospheric column (mm). Wentz and Spencer (1998) estimated a value of L from a satellite study using $0.18\times(1+(Hp)^{0.5})$, where H is the rain column depth, taken as equal to 3 km at mid latitudes. In this formulation there is no distinction between convective and stratiform precipitation. These two formulations apply to very soluble gases like HNO_3. To evaluate r for other gases, results from Crutzen and Lawrence (2000) have been used. They determined a factor α_{spec} that varies from 0 for insoluble gases to 1 for very soluble gases, and depends on the Henry's Law coefficient (see Table 2) in such way that the new local loss frequency, $r*=r\times\alpha_{spec}$ is calculated. Note that none of these wet deposition schemes make a distinction between precipitation within and below clouds. This information was not available from ECMWF analyses for this study.

Results from the runs including dry and wet deposition, S-WET1 (pink lines), S-WET2 (blue lines) and S-WET3 (green lines) are shown in Fig. 6 together with precipitation rates simulated by ECMWF along the trajectory. It can be noted that the Lagrangian matches correspond with very low precipitation which is coherent with the fact that modelled photolysis rates agree well with measured values in runs with no clouds.

In order to compare the rate of decrease of HNO_3, a parameter $\tau_{1/2}$ can be defined as $\tau_{1/2}=\log(2)\times\frac{1}{r_{mean}}$ where r_{mean} is the mean local loss frequency calculated along the trajectory. This parameter is the half-life of a trace gas corresponding to an exponential decrease in its concentration. It is equal to 19, 15 and 6 h, respectively, for simulations dry+S-WET1, dry+S-WET2 and dry+S-WET3. The run dry+S-WET3 underestimates HNO_3 concentrations by about 2.5 ppbv compared to the measurements on 21 July. Results from the dry+S-WET1 and dry+S-WET2 simulations compare better with the data even if HNO_3 is underestimated in the dry+S-WET2 run by about 1.5 ppbv on 21 July, and overestimated in the dry+S-WET1 run by the same order of magnitude.

Overall, results using ECMWF precipitation rates (S-WET2 and S-WET3) do not give better results than S-WET1 even if these schemes are more realistic. Here, and

ACPD
8, 7509–7554, 2008

in the following sections, results using wet deposition scheme, S-WET2, have been used because it gives better agreement with HNO_3 measurements than S-WET3, and is more physically realistic that S-WET1. Since NO_y is mainly made up of HNO_3, the half-life of HNO_3 with the S-WET2 scheme can be compared with the one estimated by Stohl et al. (2002) for NO_y during the 1997 NARE campaign also off the north-east coast of North America. In that study $\tau_{1/2}$ was estimated to be around 40 h, a factor of 2 slower than in the case studied here. This can be partly explained by the fact that air masses selected by Stohl et al. (2002) were rapidly exported out of the BL by frontal warm conveyor belts, and so only subject to wet deposition. The plume studied here stayed in the BL during the first few days, and was therefore influenced by both wet and dry deposition.

Overall results from the chemistry and dry/wet deposition are closer to the measurements than the chemistry only run. The impact of wet deposition is also important for other species apart from HNO_3. Modelled NO_x is now almost equal to zero after 6 days due to the loss of HNO_3. This has an impact on O_3 production rates which decrease by 60 % due to the wet removal of HNO_3. This leads to better agreement with the observations, although O_3 is still overestimated slightly and NO slightly underestimated. OH is reduced by 27% when wet deposition is included leading to a slight increase in CO lifetime from 20 to 23 days. CO is still overestimated compared to the data suggesting that dilution and mixing were also important.

4.3 Role of mixing

4.3.1 Mixing parametrisation

In the previous simulations the plume was considered isolated from the background. In the real atmosphere, a plume is subject to stirring by large-scale winds followed by mixing by processes such as turbulence. This mixing process entrains surrounding air masses leading to changes in plume concentrations. In the model, the mixing scheme is a simple linear relaxation scheme (Evans et al., 2000) resulting in an exponential

decay of plume concentrations toward background concentrations with a typical time scale, τ-mix. Because of the Lagrangian aspect of this work, measurements made in the vicinity of the plume during the 5 match segments can be used to estimate background concentrations. This method has already been applied successfully to the Lagrangian forest fire plume case sampled during ICARTT (Real et al., 2007). The values used here are summarised in Table 3. During the first 3 days, the so-called background concentrations were typical of polluted air masses. Indeed, pollutant concentrations measured by the P3 on 20, 21 and 22 July between the ground and 2 km were always elevated over the Gulf of Maine and Nova Scotia. Between 22 and 25 July, the plume left the North American east coast, and travelled over the ocean. It can be considered that after leaving the coast, the plume was no longer surrounded by polluted air masses but by marine air masses. For this reason, air masses typical of marine air, measured in proximity to the plume on 25 July, were used to characterise background air masses during this transport. Finally, high levels of NO (up to 1.5 ppbv) and NO_y (up to 6 ppbv) were measured on 26 July just after the sampling of the plume and so, higher levels of trace gases were used to define background values. These NO_y rich air masses were relatively poor in CO and O_3 but rich in NO suggesting that they could be due to local ship emissions in the English Channel (Corbett and Koehler, 2003). However, back trajectories also show transport from southern England suggesting a possible urban source.

With regard to determination of τ-mix, changes in CO concentration are often used since CO evolution is usually associated with strong dilution of polluted plumes (e.g. see Real et al., 2007). However, in this case, the decrease in CO is strongly influenced by photochemical processes, and so, is not a very good indicator of mixing. Arnold et al. (2006) evaluated a τ of 10 days with a method based on hydrocarbon ratio changes, for plumes crossing the North Atlantic during the ICARTT campaign. The same τ was used here except for the last day when a faster mixing rate was used (τ=2 days) as soon as the plume entered the European BL, to represent the strong increase in NO and NO_y observed on the 26 July. It should be noted that the CO values mea-

ACPD
8, 7509–7554, 2008

sured on the 26 July in the vicinity of the plume are very close to the value in the plume itself. On this day, the plume was not easily distinguishable from the background based on CO or O_3 measurements alone. The mixing time-scale of 10 days, used during the first 5 days, implies slightly weaker mixing rates compared to previous studies (Real et al., 2007; Price et al., 2004). This could be related to the plume remaining relatively intact during transport due to strongly converging low level winds, and the fact that the plume was decoupled from the marine BL during transport making mixing and dilution less important in this case. However, the impact of the chosen value for the mixing rate is strongly dependent on the background mixing values used. For example, applying a stronger mixing rate during the first 3 days would not change results by much as the chosen background values are similar to those in the plume. The chosen mixing rates are therefore linked to a particular definition of the geographical limits of the plume, and should not therefore be taken as representative values for the lower atmosphere.

4.3.2 Results: chemistry, deposition and mixing

Model results including chemistry, deposition and mixing processes are shown in Fig. 8. During the first 5 days, mixing does not change concentrations very much, mainly because of the low mixing rates used, and the fact that background concentrations used during the first 3 days are not much different from those in the plume. Overall, there is now good general agreement between the model simulations and the measurements for the entire period except for 22 July, which supports the hypothesis that this day is not a truely Lagrangian match. The agreement on the 21 is generally good although NO which is still slightly underestimated. There is good agreement with CO and O_3 data on 25 July, with further decreases of 13 and 6 ppbv, respectively, but NO is still underestimated. However, as the measured NO value is so low that it is close to the detection limit of the instrument it is hard to come to any conclusion on the overestimation or not by the model. Modelled concentrations are also closer to the data on the 26 July, especially for NO which was mixed with higher background values. These discrepancies are analysed further in the following section using O_3/CO and NO_y/CO

correlations.

Concerning the modelled OH values, the runs including deposition and mixing lead to a reduction in OH of 25% with a mean values of 3×10^6 molecs. cm^{-3} over the period from the 21 to 25 July, with peak noon values around 14×10^6 molecs. cm^{-3}. These values are still slightly higher than measurements from George et al. (1999) in recent polluted plumes but in better agreements with the ones of Ehhalt and Roher (2000). Moreover, since the *J*-values and O_3 data agree well we can have some confidence in OH results.

It is also interesting to re-examine the comparison with measured VOCs. Whereas all VOCs measured on 25 July were underestimated in the run with chemistry only, the model results including deposition and mixing for the long lived VOCs are now in better agreement with the data mainly because of the decrease in modelled OH. For example, on 25 July, the comparisons are 1076 pptv, 159 pptv and 22 pptv for modelled C_2H_6, C_2H_2 and C_4H_10 against measured values of 1075 pptv, 169 pptv and 25 pptv, respectively. On the other hand, modelled values of C_2H_4 and C_3H_6 with shorter lifetimes of 2 and 0.8 days are almost zero when measurements show values around 100 pptv for this two species. It is possible that the plume was influenced by local oceanic or biogenic emissions of these species off the coast of Ireland. Such air masses with elevated emission of alkenes and low CO and O_3 values were measured in proximity to the Lagrangian plume by the Falcon.

Further light is shed on this in the next section comparing modelled and measured trace gas correlations (see Sect. 4.4).

4.3.3 Influence of the different processes on pollutant levels in the plume

By analysing simulated O_3 production and destruction terms, the influence of chemical, deposition and mixing processes on O_3 can be evaluated. In the runs including all processes, and giving the best agreement with the data, a decrease of 42 ppbv in O_3 concentrations over 6 days is calculated. Of this decrease 75% is due to chemical destruction, including the effects of dry and wet deposition on O_3 production, which

gives a mean net O_3 production of –5 ppbv/day. The remaining 25% is due to direct O_3 dry deposition (10%) and mixing (15%). Without both wet and dry deposition the net O_3 production is only –1.1 ppbv/day. This is mainly due to HNO_3 photolysis providing a source of NO_x as discussed previously. Thus, these model results show that indirectly deposition processes were responsible for 80% of the impact of photochemistry on O_3, with the large majority (78%) being due to wet deposition rather than dry deposition. Modelled CO decreases by 60 ppbv which is in good agreement with the observed evolution in the plume. Analysis of model results shows that 66% is due to chemical destruction and 34% due to mixing and dilution of the plume. Therefore, in this case, photochemical processes governed the evolution of both O_3 and CO in the plume. Whilst this has been shown previously to be the case for O_3, this is the first time, to our knowledge, that photochemistry has been shown to be the dominant process governing CO evolution over a period of several days. If the plume had not been subject to deposition processes, it would have reached Europe with much higher levels of O_3 (80–90 ppbv), and lower levels of CO (120–140 ppbv). It can be envisaged, that plumes originating from North America with slightly lower CO values, would reach Europe with even lower CO values due to strong OH oxidation, and thus may not be detected using the methods often applied to diagnose pollutant plumes such as application of CO thresholds. This point is discussed further in the next section.

4.4 Correlation study

Comparison of the full range of observed and simulated concentrations in the Lagrangian match samplings, and their interelationships can provide useful additional information about the evolution of pollutant concentrations in a plume, than just comparison of means ±std. Observed correlations in the Lagrangian matches have already been discussed in Sect. 2. In this section, multiple runs are used in order to characterise the variability across the Lagrangian samplings in an attempt to reproduce the observed changes in the correlation between species.This method has already been used successfully to analyse the forest fire case sampled during ICARTT (Real et al.,

2007).

The multiple model runs were initialised with P3 measurements averaged every 30s during 20 July Lagrangian match samplings. With this method, each run represents a different part of the initial correlation (black crosses in Fig. 9) observed by the P3. Model results after 1 (green triangles), 2 (blue diamonds), 4 (pink squares) and 5 (violet stars) days are shown in Fig. 9 for 3 cases: chemistry-only simulations (case A), simulations with chemistry and wet plus dry deposition (case B), and simulations with chemistry, deposition and mixing (case C). O_3/CO and NO_y/CO correlations are shown for each case, and NO/CO correlations are shown for case C. The simulated slopes for the different cases are reported in Table 4.

It has already been seen in Sect. 4.1 that the chemistry-only runs were unable to reproduce the chemical evolution of the plume but, nevertheless, it is still interesting to examine the evolution of the slopes in the case without deposition or mixing. The O_3/CO and NO_y/CO simulated in case A are very different from those observed. The slopes increase with time whereas the data show an overall decrease. The modelled increase is not due to an increase in NO_y or O_3 that remains nearly constant, but is due to the strong chemical destruction of CO in these runs. Therefore, in the run with chemistry only, an increase in the O_3/CO slope is the result of a decrease in CO, and not the result of photochemical O_3 production as it is often stated (Andreae et al., 1994; Mauzerall et al., 1998). Along the same lines, Chin et al. (1994) showed that a decrease in O_3/CO slope could be due to the secondary production of CO by hydrocarbon oxidation in a fresh plume, and not only due to chemical destruction or deposition of O_3. When deposition processes are included (case B), NO_y/CO slopes show very good agreement with those observed on 21 and 25 July but not on 26 July. Modelled O_3/CO slopes now decrease but less than observed on the 25 July. Because mixing is simulated as a homogeneous process, modelled slopes change little between cases B and C due to small changes in O_3 production. However, the correlation lines are shifted towards "background" concentrations, and the dispersion is reduced (see also discussion in Real et al., 2007). This leads to better overall agreement with the

data in this correlation space although there are still some differences. The bad match between measurements and simulations on the 22 July has already been identified using mean concentrations analysis (Sect. 4.1) and is not discussed further.

Interestingly, this approach shows differences for the 25 July in measured and modelled O_3/CO slopes (–0.03 and 0.36, respectively) that were not apparent in the simulations using mean concentrations which agree well with the mean data. Further analysis based on the correlations suggests that the measurements in this Lagrangian match can be divided into 2 different parts, from 15:54 to 16:06 and 16:06 to 16:21, and 2 different air masses may have in fact been sampled. This distinction is shown in Fig. 10 based on the observed O_3/CO correlation. For the first segment, CO and O_3 are not really correlated, with a slope of 0.02 whereas for the second segment, the slope is positive with a value of 0.28, and a correlation coefficient of 0.75. This slope is comparable to measured values at ground-based sites such as Mace Head (Li et al., 2002). It is also closer to the simulated slope (0.36) whereas the weak slope in the first segment is not reproduced by the model runs initialised with measurements on 20 July. Therefore, it seems that the second segment represents the best match with the plume from 20 July whereas the first segment appears to have been influenced by inhomogeneous mixing in the edges of the plume, possibly with marine air masses, not reproduced by the model.

The last important difference is observed between modelled and measured NO/CO and NO_y/CO slopes between the 25 and 26 July. The data slopes are particularly strong on the 26 July, especially compared to the 25 July. In this case the Lagrangian plume appears to have been strongly dispersed when it reached Europe on the 26 July and "background" concentrations also included fresh emissions with very high levels of NO and NO_y, as noted previously. The model does not capture this variability since the plume is not mixed with the full range of concentrations in this local plume but only with its mean concentrations. Therefore, this last sampling cannot be really considered as Lagrangian because of the strong influence of fresh emissions.

ACPD
8, 7509–7554, 2008

5 Conclusions

The case of an anthropogenic plume transported from North America (New York-Boston region) over the North Atlantic to Europe at low altitudes has been studied in a Lagrangian framework. This plume was initially strongly polluted with high concentrations of O_3, CO and NO_x, typical of North American polluted plumes, and also very high levels of HNO_3. During transport, all pollutant concentrations decreased, and the plume was much less polluted when it was intercepted off the west coast of Ireland several days later. A Lagrangian photochemical model (CiTTyCAT), has been used to assess the different processes influencing the evolution of pollutant levels in the plume during this long-range transport. Average concentrations and correlations between trace species (O_3/CO and NO_y/CO) were examined, and compared to data collected in the Lagrangian match segments. Overall, the analysis shows that some of the links identified as Lagrangian by Methven et al. (2006) are not truly Lagrangian, in particular for 22 July because of probable errors in ECMWF coastal winds and 26 July due to the influence of local emissions. In addition the correlation analysis showed that part of the match on 25 July also appears not to be well linked to 20 July.

The evolution of the chemical composition in the plume (mean values and correlations lines) is best reproduced when photochemistry, dry/wet deposition and mixing with surrounding air masses are all included. Model results show that these changes were mainly driven by photochemical and deposition processes, especially wet deposition. Mixing with air masses in close proximity to the plume during transport did not have a strong impact on trace gas concentrations during the first 5 days due to strong and rapid transport by low level winds and isolation of the plume from the marine boundary layer over the Atlantic. Mixing with local pollution sources (from ships or London connurbation) appears to have been important on the 26 July.

Mean net O_3 production in the plume was negative over the 6 day period at about –5 ppbv/day leading to mean O_3 plume level of 44 ppbv when it reached Europe. This value is low compared to European pollution over land but is significantly enhanced

ACPD
8, 7509–7554, 2008

compare to the remote oceanic region where the plume was sampled. Plume O_3 was directly impacted by dry deposition, and indirectly by wet deposition through the strong scavenging of HNO_3. For the plume studied here, this implies that wet deposition was responsible for an 80% reduction in net O_3 production. This study and the one from Neuman et al. (2006) show that because polluted plumes from the New-York/Boston region were very rich in HNO_3, wet deposition can have a strong impact on O_3 levels. Runs with no wet deposition, showed that HNO_3 photolysis can maintain high O_3 levels during plume transport leading to much lower mean net loss (–1 ppbv/day). In that case, the plume would have reached Europe with much higher O_3 levels (between 80 and 90 ppbv) resulting in a strong import of O_3 directly in the European BL.

Another important result is the important influence of photochemistry on CO levels in the plume rather than mixing which is usually assumed to be the most important process over this time scale. In this case, photochemical destruction explains 66% of the CO decrease compared to only 34% for mixing. This is due to relatively high O_3 levels coupled with high water vapour levels leading to a high oxidising capacity in the plume, and therefore a reduction of CO chemical lifetime to 23 days. This has several consequences. Firstly, this means that CO cannot be always used as a tracer of North American pollution when the plume transport is at low altitudes. This may also explain the low levels of CO often observed in the European BL in plumes originating from North America. The latter does not imply that the plume was weakly polluted but that photochemistry was intense. Secondly, we have shown that an observed increase in the O_3/CO correlation slope can result from CO chemical oxidation (destruction), and not photochemical production of O_3 as is often assumed.

Overall, these results show that O_3 import into downwind regions can be very sensitive to scavenging processes along route as well as photochemical processing and that CO levels can also be strongly influenced by photochemical loss. Whilst there are uncertainties related to the Lagrangian analysis including errors in trajectories, studies using this modelling framework are able to provide detailed analysis of the processes governing pollutant levels during long-range transport. They can also be used to eval-

uated plume transport and processing in global models that typically have problems resolving such features.

Acknowledgements. E. Real and K. Law acknowledge financial support from national programmes (PNCA, PATOM) provided by INSU, ADEME and also from Insitut Pierre Simon Laplace (IPSL) for the French ITOP project as well as the Institut Geographique National (IGN) for hosting the DLR Falcon campaign at Creil, France. We would like to thank the whole ICARTT team, and in particular P3 scientists.

References

Andreae, M. O., Anderson, B. E., Blake, D. R., Bradshaw, J. D., Collins, J. E., Gregory, G. L., Sachse, G. W., and Shipham, M. C.: Influence of plumes from biomass burning on atmospheric chemistry over the equatorial and tropical South Atlantic during CITE3, J. Geophys. Res., 99, 12,793–12,808, 1994. 7532

Arnold, S. R., Methven, J., Evans, M. J., Chipperfield, M. P., Lewis, A. C., Hopkins, J., McQuaid, J. B., Watson, N., Purvis, R. M., Lee, J. D., Atlas, E. L., Blake, D. R., and Rappenglck, B.: Quantification of mean OH concentration and air mass dilution rates from successive observations of non-methane hydrocarbons in single air masses, J. Geophys. Res., 112, D10S40, doi:10.1029/2006JD007594, 2006. 7519, 7528

Auvray, M. and Bey, I.: Long-range transport to Europe: Seasonal variations and implications for the European ozone budget, J. Geophys. Res., 110, D11 303, doi:10.1029/2004JD005503, 2005. 7512

Brown, S. S., Ryerson, T. B., Wollny, A. G., Brock, C. A., Peltier, R., Sullivan, A. P., Weber, R. J., Dub, W. P., Trainer, M., Meagher, J. F., Fehsenfeld, F. C., and Ravishankara, A. R.: Variability in nocturnal nitrogen oxide processing and its role in regional air quality, Science, 311, 67–70, 2006. 7521

Chen, M., Talbot, R., Mao, H., Sive, B., Chen, J., and Griffin, R. J.: Air mass classification in coastal New England and its relationship to meteorological conditions., J. Geophys. Res., 112, D10S05, doi:10.1029/2006JD007687, 2007. 7517

Chin, M., Jacob, D., Munger, J. W., Parrish, D. D., and Doddridge, B. G.: Relationship of ozone and carbon monoxide over North America, J. Geophys. Res., 99, 14 565–14 573, 1994. 7532

Corbett, J. J. and Koehler, H. W.: Updated emissions from ocean shipping., J. Geophys. Res., 108, 4650, 2003. 7528

Crutzen, P. J. and Lawrence, M. G.: The impact of precipitation scavenging on the transport of trace gases: A 3-dimensional model sensitivity study, J. Atmos. Chem., 37, 81–112, 2000. 7526

Derwent, R. G., Richard, G., Jenkin, M. E., Saunders, S. M., and Pilling, M. J.: Photochemical ozone creation potentials for organic compounds in northwest Europe calculated with a master chemical mechanism., Atmos. Environ., 32, 2429–2441, 1998. 7511

Derwent, R. G., Ollins, D. S. S. W. J., and Johnson, E.: Intercontinental transport and the origins of the ozone observed at surface sites in Europe., Atmos. Environ., 38, 1891–1901, 2004. 7512

Ehhalt, D. and Roher, F.: Dependence of the OH concentration on solar UV., J. Geophys. Res., 105, 3565–3571, 2000. 7523, 7530

Evans, M. J., Shallcross, D. E., Law, K. S., Wild, J. O. F., Simmonds, P. G., Spain, T. G., Berrisford, P., Methven, J., Lewis, A. C., McQuaid, J. B., Pillinge, M. J., Bandyf, B. J., Penkett, S. A., and Pyle, J. A.: Evaluation of a Lagrangian box model using field measurements from EASE (Eastern Atlantic Summer Experiment) 1996, Atmos. Environ., 34, 3843–3863, 2000. 7519, 7520, 7527

Fehsenfeld, F., Ancellet, G., Bates, T., Goldstein, A., Hardesty, M., Honrath, R., Law, K., Lewis, A., Leaitch, R., McKeen, S., Meagher, J. F., Pszenny, A., Russell, P., Schlager, H., Seinfeld, J., Trainer, M., Talbot, R., and Zbinden, R.: International Consortium for Atmospheric Research on Transport and Transformation (ICARTT) - North America to Europe: Overview of the 2004 summer field study, J. Geophys. Res., 111, D23S01, doi:10.1029/2006JD007829, 2006. 7512, 7516

George, L. A., Hard, T. M., and O'Brian, R. J.: Measurements of free radicals OH and HO_2 in Los Angeles smog, J. Geophys. Res., 104, 11 643–11 655, 1999. 7523, 7530

Guerova, G., Bey, I., Atti, J.-L., Martin, R. V., Cui, J., and Sprenger, M.: Impact of transatlantic transport episodes on summertime ozone in Europe, Atmos. Chem. Phys., 6, 2057–2072, 2006, http://www.atmos-chem-phys.net/6/2057/2006/. 7516

Honrath, R. E., Owen, R. C., Martin, M. V., Reid, J. S., Lapina, K., Fialho, P., Dziobak, M. P., Kleissl, J., and Westphal, D. L.: Regional and hemispheric impacts of anthropogenic and biomass burning emissions on summertime CO and O_3 in the North Atlantic lower free tro-

posphere., J. Geophys. Res., 109, D24310, doi:10.1029/2004JD005147, 2004. 7517
Hough, A.: The calculation of photolysis rates for use in global troposheric modeling studies, Tech. rep., Energy Res. Estab., Her Majesty's Stn. Off., London, 1988. 7519
Huntrieser, H., Heland, J., Schlager, H., Forster, C., Stohl, A., Aufmhoff, H., Arnold, F., Scheel, H. E., Campana, M., Gilge, S., Eixmann, R., and Cooper, O.: Intercontinental air pollution transport from North America to Europe: Experimental evidence from airborne measurements and surface observations., J. Geophys. Res., 110, D01305, doi:10.1029/2004JD005045, 2005. 7511
Li, Q., Jacob, D. J., Bey, I., Palmer, P., Duncan, B. N., Field, B. D., Martin, R. V., Fiore, A. M., Yantosca, R. M., Parrish, D. D., Simmonds, P. G., and Oltmans, S. J.: Transatlantic transport of pollution and its effects on surface ozone in Europe and North America., Atmos. Environ., 107(D13), 4166, doi:10.1029/2001JD001422, 2002. 7511, 7512, 7516, 7518, 7533
Li, Q., Jacob, D. J., Park, R., Wang, Y., Heald, C., Hudman, R., Yantosca, R., Martin, R., and Evans, M.: North American pollution outflow and the trapping of convectively lifted pollution by upper-level anticyclone., J. Geophys. Res., 110, D10301, doi:10.1029/2004JD005039, 2005. 7511, 7515, 7516
Mauzerall, D. L., Logan, J. A., Jacob, D. J., Anderson, B. E., Blake, D. R., Bradshaw, J. D., Haikes, B., Sachse, G. W., Singh, H., and Talbot, B.: Photochemistry in biomass burning plumes and implications for tropospheric ozone over the tropical South Atlantic, J. Geophys. Res., 103, 8401–8423, 1998. 7532
Methven, J., Arnold, S. R., Stohl, A., Avery, M., Law, K., Lewis, A., Parrish, D., Reeves, C., Schlager, H., Atlas, E., Blake, D., and Rappenglck, B.: Establishing Lagrangian connections between observations within air masses crossing the Atlantic during the ICARTT experiment, J. Geophys. Res., 111, D23S62, doi:10.1029/2006JD007540, 2006. 7513, 7514, 7515, 7516, 7518, 7519, 7534, 7541
Millet, D. B., Goldstein, A. H., Holzinger, R., Williams, B. J., Allan, J. D., Jimenez, J. L., Worsnop, D. R., Roberts, J. M., White, A. B., Hudman, R. C., Bertschi, I. T., and Stohl, A.: Chemical characteristics of North American surface layer outflow: Insights from Chebogue Point Nova Scotia, J. Geophys. Res., 111, D23S53, doi:10.1029/2006JD007287, 2006. 7511
Neuman, J. A., Parrish, D. D., Trainer, M., Ryerson, T. B., Holloway, J. S., Nowak, J. B., Swanson, A., Flocke, F., Roberts, J. M., Brown, S. S., Stark, H., Sommariva, R., Stohl, A., Peltier, R., Weber, R., Wollny, A. G., Sueper, D. T., Hubler, G., and Fehsenfeld, F. C.: Reactive nitrogen transport and photochemistry in urban plumes over the North Atlantic Ocean, J.

Geophys. Res., 111, D23S54, doi:10.1029/2005JD007010, 2006. 7524, 7535
Owen, R. C., Cooper, O. R., Stohl, A., and Honrath, R. E.: An analysis of the mechanisms of North American pollutant transport to the central North Atlantic lower free troposphere., J. Geophys. Res., 111, D23S58, doi:10.1029/2006JD007062, 2006. 7511
Parrish, D. D., Holloway, J. S., Trainer, M., Murphy, P. C., Forbes, G. L., and Fehsenfeld, F. C.: Relationship between ozone and carbon monoxide at surface sites in the North Atlantic region, J. Geophys. Res., 103, 13 357–13 376, 1998. 7511, 7517
Penner, J. E., Atherton, C. S., Dignon, J., Ghan, S. J., and Walton, J. J.: Tropospheric nitrogen: a three-dimensional study of sources, distribution and deposition, J. Geophys. Res., 96, 959–990, 1991. 7525
Price, H. U., Jaffe, D. A., Cooper, O. R., and Doskey, P. V.: Photochemistry, ozone production, and dilution during long-range transport episodes from Eurasia to the northwest United States, J. Geophys. Res., 109, D23S13, doi:10.1029/2003JD004400, 2004. 7529
Real, E., Law, K. S., Wienzierl, B., Fiebig, M., Petzold, A., Wild, O., Methven, J., Arnold, S., Stohl, A., Huntrieser, H., Roiger, A., Schlager, H., Stewart, D., Avery, M., Sachse, G., Browell, E., Ferrare, R., and Blake, D.: Processes influencing ozone levels in Alaskan forest fires plumes during long-range transport over the North Atlantic, J. Geophys. Res., 112, D10S41, doi:10.1029/2006JD007576, 2007. 7514, 7515, 7519, 7528, 7529, 7531, 7532
Riddle, E. E., Voss, P. B., Stohl, A., Holcomb, D., Maczka, D., Washburn, K., and Talbot, R. W.: Trajectory model validation using newly developed altitude-controlled balloons during the International Consortium for Atmospheric Research on Transport and Transformations 2004 campaign, J. Geophys. Res., 111, D23S57, doi:10.1029/2006JD007456, 2006. 7515
Rossow, W. B. and Schiffer, R. A.: ISCCP cloud data products, Bull. Am. Meteorol. Soc., 72, 2–20, 1991. 7523
Schubert, S. D., Rood, R. B., and Pfaendtner, J.: An assimilated data set for earth science applications, Bull. Am. Meteorol. Soc., 74, 2331–2342, 1993. 7520
Stohl, A.: A 1-year Lagragian "climatology" of airstreams in the Northern hemisphere troposphere and lowermost stratosphere, J. Geophys. Res., 106, 7263–7279, 2001. 7511
Stohl, A., Wotawa, G., Seibert, P., and Kromp-Kolb, H.: Interpolation errors in wind fields as a funcion of spatial and temporal resolution and their impact on different types of kinematic trajectories, J. Appl. Meteorol., 34, 2149–2165, 1995. 7520
Stohl, A., Eckhardt, S., Forster, C., James, P., and Spichtinger, N.: On the pathways and timescales of intercontinental air pollution transport, J. Geophys. Res., 107(D23), 4684,

doi:10.1029/2001JD001396, 2002. 7511, 7512, 7527
Stohl, A., Cooper, O. R., Damoah, R., Fehsenfeld, F. C., Forster, C., Hsie, E.-Y., Hbler, G., Parrish, D. D., and Trainer, M.: Forecasting for a Lagrangian aircraft campaign, Atmos. Chem. Phys., 4, 1113–1124, 2004,
http://www.atmos-chem-phys.net/4/1113/2004/. 7514
Walton, J. J., Maccracken, M. C., and Ghan, S. J.: A global-scale lagrangian trace species model of transport, transformation, and removal processes, J. Geophys. Res., 93, 8339–8354, 1988. 7525
Warneke, C., de Gouw, J. A., Goldan, P. D., Kuster, A. C., Williams, E. J., Lerner, B. M., Jakoubek, R., Brown, S. S., Stark, H., Aldener, M., Ravishankara, A. R., Roberts, J. M., Marchewka, M., Bertman, S., Sueper, D. T., McKenne, S. A., Meagher, J. F., and Feshenfeld, F. C.: Comparison of daytime and nightime oxidation of biogenic VOCs along the New England coast in summer during New England Air Quality Study 2002., J. Geophys. Res., 109, D10309, doi:10.1029/2003JD004424, 2004. 7523
Wentz, F. J. and Spencer, R. W.: SSMI/I rain retrievals within a unified all-weather ocean algorithm, J. Atmos. Sci., 55, 1149–1152, 1998. 7526
Wild, O. and Akimoto, H.: Intercontinental transport of ozone and its precursors in a three-dimensional global CTM, J. Geophys. Res., 106, 27 729–27 744, 2001. 7511
Wild, O., Law, K. S., McKenna, D. S., Bandy, B. J., Penkett, S. A., and Pyle, J. A.: Photochemical trajectory modeling studies of the North Atlantic region during August 1993, J. Geophys. Res., 101, 29 269–29 288, 1996.
7519, 7520

Table 1. Measurements taken during Lagrangian match windows as defined in Table 1 of Methven et al. (2006). Data for each window is shown as "mean (standard deviation) [number of measurement averaged]". NO_y values indicated for the first 3 Lagrangian matches are simply the sum of measured HNO_3, PAN, NO_2 and NO. All measurements indicated in the first column (20 July) are used to initialise the model, exept for temperature, water vapour (ECMWF data are used) and aerosols (no aerosols in the model).

	P3-20/07 (25 mn)	P3-21/07 (6 mn)	P3-22/07 (23 mn)	Falcon-25/07 (27 mn)	Falcon-26/07 (9 mn)
CO (ppbv)	200 (30) [1427]	183 (12) [361]	181 (8) [755]	138 (12) [1621]	121 (1.8) [541]
O_3 (ppbv)	90 (15) [1501]	88 (6) [361]	57 (6) [781]	44 (2.9) [1621]	43 (1.5) [541]
NO (pptv)	63 (25) [1351]	46 (7) [361]	32 (10) [751]	10 (0.002) [1313]	47 (43) [389]
NO_2 (pptv)	441 (185) [1351]	210 (51) [361]	115 (35) [751]		
PAN (pptv)	649 (331) [650]	481 (134) [181]	268 (70) [215]		
HNO_3 (pptv)	14400 (9500) [1236]	4584 (1032) [361]	2229 (631) [646]		
NO_y (pptv)	15553 (10360)	5307 (1383)	2644 (742)	175 (38)	940 (417)
C_2H_4 (pptv)	21 (9) [5]	30 [1]	83 [2]	100 [2]	113 [2]
C_2H_6 (pptv)	1291 (303) [5]	1170 [1]	1205 [2]	1075 [2]	988 [2]
C_2H_2 (pptv)	311 (153) [5]	310 [1]	266 [2]	169 [2]	174 [2]
C_3H_6 (pptv)	3 (1) [3]	5 [1]	26 [2]	93 [2]	81 [2]
C_4H_10 (pptv)	141 (75) [5]	103 [1]	209 [2]	25 [2]	62 [2]
C_5H_8 (pptv)	0.2 (0.055) [5]	0.4 [1]	318 [2]		
C_5H_12 (pptv)	77 (35) [5]	76 [1]	94 [2]		
C_6H_6 (pptv)	61 (41) [5]	58 [1]	46 [2]		
C_7H_8 (pptv)	61 (41) [5]	24 [1]	20 [2]		
Methanol (pptv)	2197 (303) [68]	2140 (218) [14]	3360 (513) [39]		
Acetaldehyde (pptv)	758 (162) [68]	632 (82) [14]	608 (70) [39]		
Acetone (pptv)	2946 (647) [68]	2641 (187) [14]	3099 (193) [39]		
Aerosols (cm^{-3})	5474 (1646) [1501]	3627 (640) [361]	2989 (340) [751]		
Temp (K)	293 (0.2) [1501]	291 (0.3) [361]	295 (0.8) [781]	283 (0.9) [1320]	282 (0.4) [541]
H_2O (g/kg)	11.8 (0.5) [1501]	10.8 (0.5) [361]	12.8 (0.5) [781]	9.2 (0.5) [1621]	7.8 (0.3) [541]

ACPD
8, 7509–7554, 2008

Table 2. α_{spec} values as a function of effective Henry's Law coefficient.

Hf	Hf<10^3	10^3<Hf<10^4	10^4<Hf<10^5	10^5<Hf¡10^6	10^6<Hf<10^8	Hf>10^8
α_{spec}	0	0.15	0.5	0.85	0.95	1

ACPD
8, 7509–7554, 2008

Table 3. Measured concentrations in the vicinity of the Lagrangian plume used as background concentrations for the mixing simulations.

Time windows	CO (ppbv)	O_3 (ppbv)	NO_y (pptv)	NO (pptv)
21:00, 20 July–12:00, 21 July	182	73	6109	120
21:00, 21 July–12:00, 22 July	184	78	4085	55
12:00, 22 July–12:00, 23 July	170	65	3502	42
12:00, 23 July–22:00, 25 July	90	30	150	10
22:00, 25 July–26, July	130	47	5910	1160

Table 4. Measured and simulated O_3/CO correlation slopes with and without mixing and deposition. Measured correlation coefficients *r* are also reported in brackets.

	Measured slopes	Simulated without mixing or deposition (Case a)	Simulated with deposition (Case b)	Simulated with deposition and mixing (Case c)
P3–20 : O_3/CO	0.47 (0.91)			
: NO_y/CO	0.31 (0.85)			
: NO/CO	0.74 (0.89)			
P3–21 : O_3/CO	0.51 (0.93)	0.52	0.46	0.46
: NO_y/CO	0.09 (0.85)	0.27	0.09	0.09
: NO/CO	0.08 (0.14)	0.4	0.17	0.17
P3–22 : O_3/CO	0.17 (0.21)	0.59	0.45	0.45
: NO_y/CO	0.02 (0.3)	0.29	0.05	0.05
: NO/CO	0.16 (0.14)	0.41	0.09	0.09
Falcon 25 : O_3/CO	–0.03 (–0.12)	0.69	0.36	0.37
: NO_y/CO	0.001 (0.32)	0.3	0.0015	0.0015
: NO/CO	0.09 (0.043)	0.41	0.013	0.013
Falcon 26 : O_3/CO	–0.31 (–0.35)	0.66	0.33	0.33
: NO_y/CO	0.14 (0.7)	0.27	0.0011	0.0011
: NO/CO	15.5 (0.76)	0.23	0.009	0.009

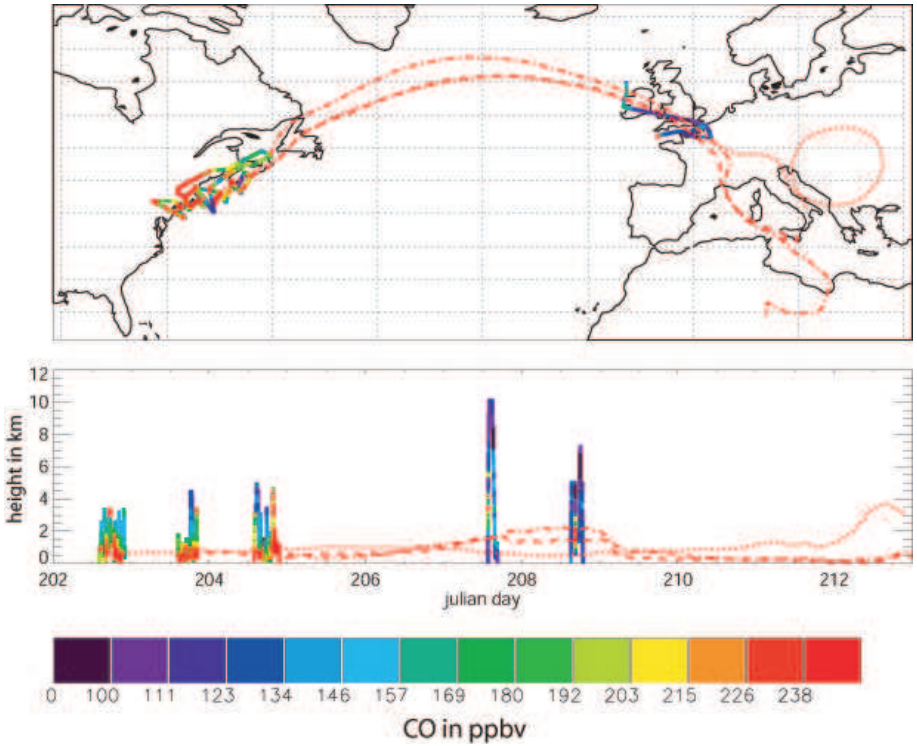

Fig. 1. Flight tracks of the P3 flights on the 20, 21, 22 July 2004 and Falcon flight on the 25 and 26 July 2004, coloured with measured CO. Three forward trajectories initialised in the 3 Lagrangian samplings of the P3 are also represented (respectively dotted, dashed and dashed-dotted lines on 20, 21 and 22 July 2004).

ACPD
8, 7509–7554, 2008

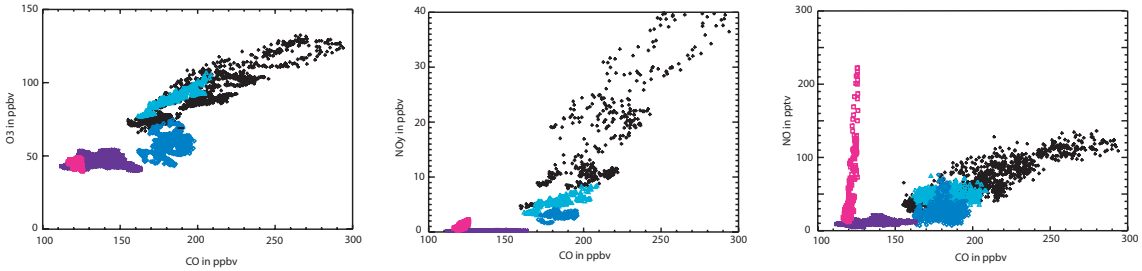

Fig. 2. Measured O_3 and reactive nitrogen concentrations (NO,NO_y) versus measured CO in the 5 Lagrangian match samplings. Black crosses represent measurements taken on 20 July and light blue triangles, dark blue diamonds, violet stars and pink squares the measurements taken on 21, 22, 25 and 26 July 2004, respectively.

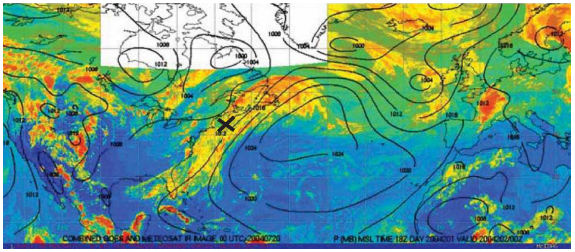

20 July

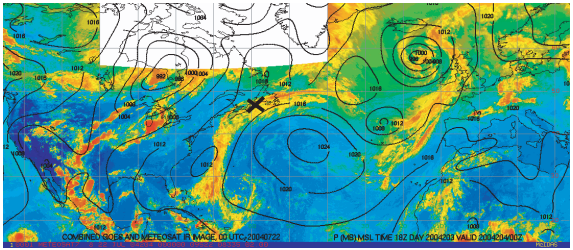

22 July

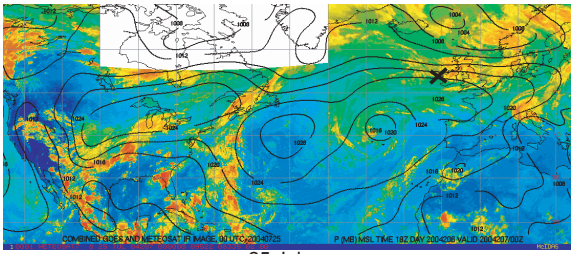

25 July

Fig. 3. Infrared images combined from GEOS and METEOSAT for 20, 22 and 25 July 2004 taken from the NOAA products in support of ICARTT (Courtesy of O. Cooper, NOAA ESRL). Ground pressure values (black lines isobars) are also indicated. Black crosses represent the location of the Lagrangian matches on each day.

ACPD

8, 7509–7554, 2008

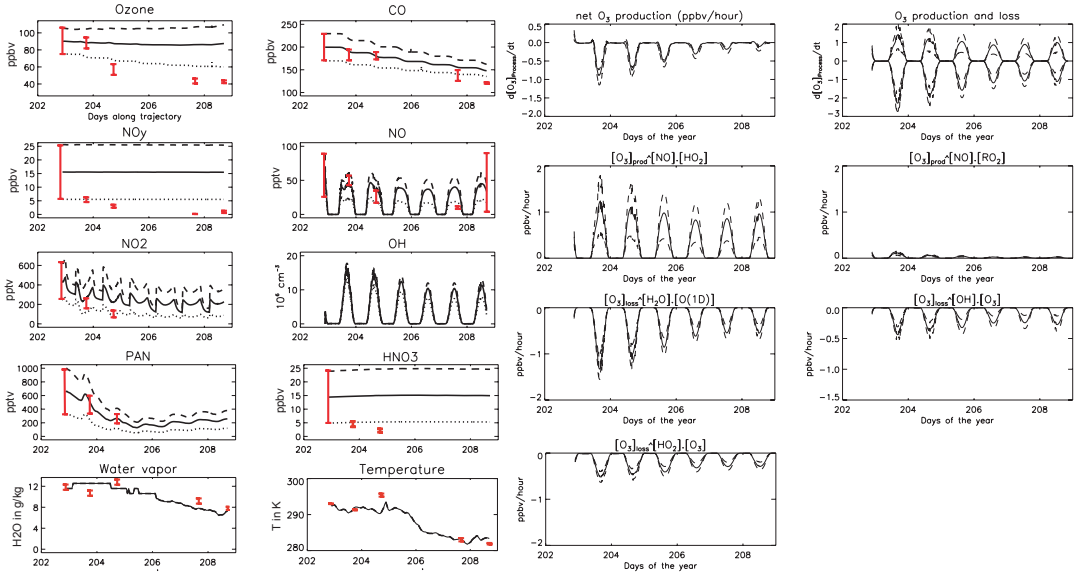

(a) Concentrations, water vapour and temperature (b) Hourly O_3 production and destruction terms

Fig. 4. Temporal evolution of **(a)** simulated concentrations, and **(b)** simulated O_3 production and destruction rates, initialised with mean (continuous lines), mean –std (dotted line) and mean +std (dashed lines) concentrations taken from the P3 measurements on 20 July. Downwind mean and std measurements taken in the plume are represented as red vertical lines (see text for details).

ACPD
8, 7509–7554, 2008

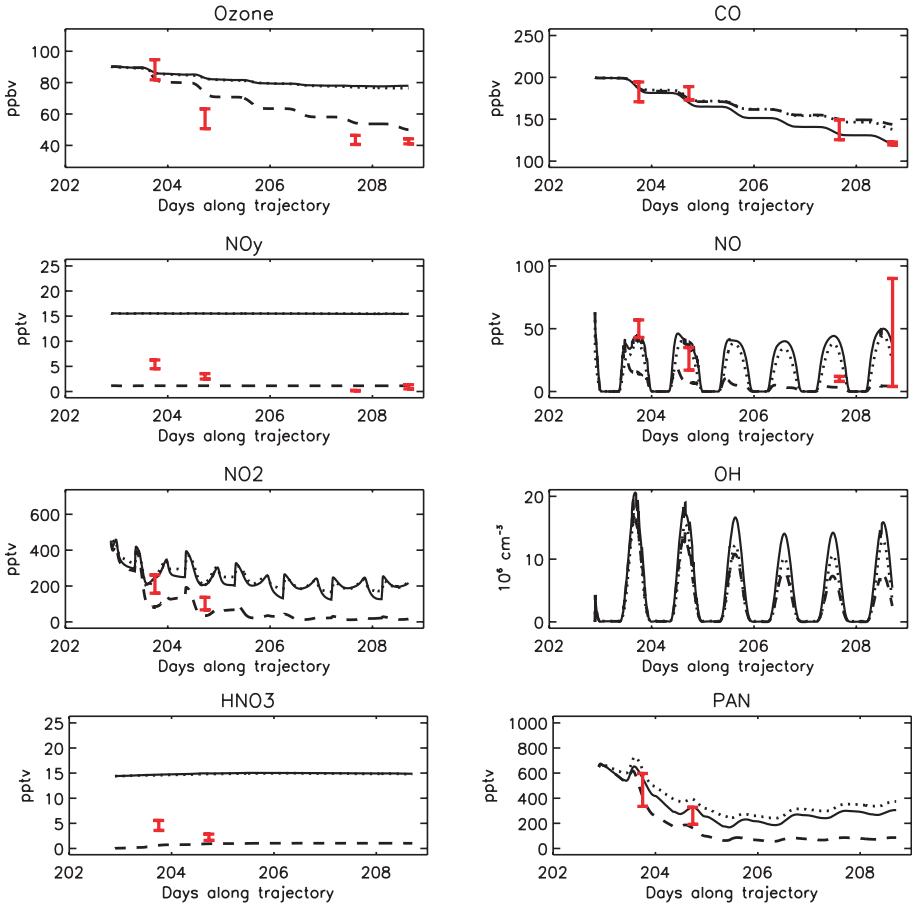

Fig. 5. Reference simulation (continuous lines), S-noHNO_3 simulation (dashed lines) and S-CLOUD simulation (dotted lines) (see text for details).

ACPD
8, 7509–7554, 2008

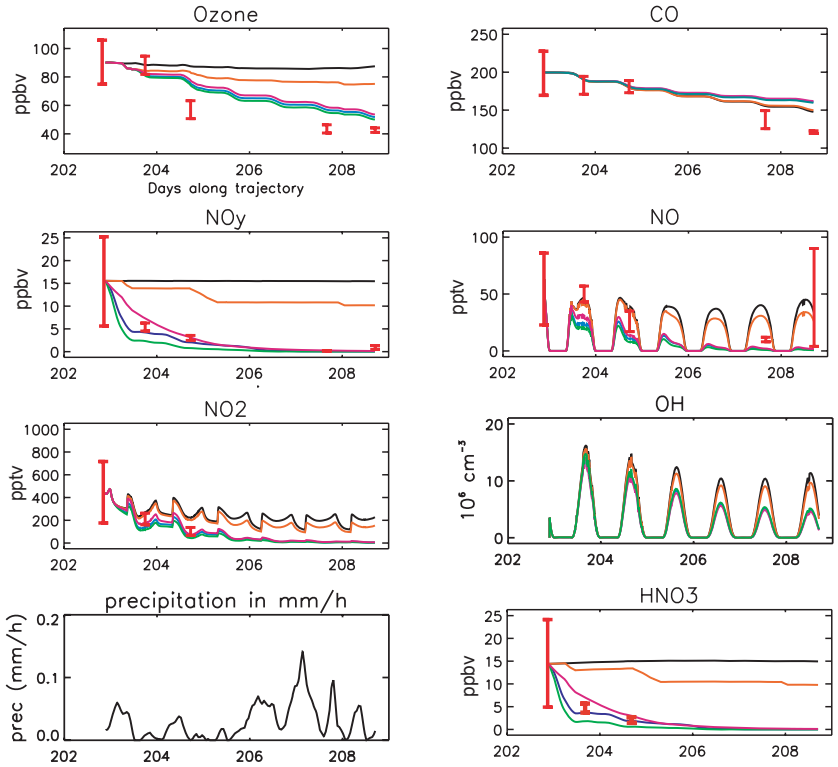

Fig. 6. Simulation without deposition (black lines), with dry deposition only (orange lines), with S-WET1 wet deposition+dry deposition (pink lines), with S-WET2 wet deposition+dry deposition (bllue lines), and with S-WET3 wet deposition+dry deposition (green lines). Precipitation interpolated from ECMWF precipitation rates (sum over total column) are also shown.

ACPD
8, 7509–7554, 2008

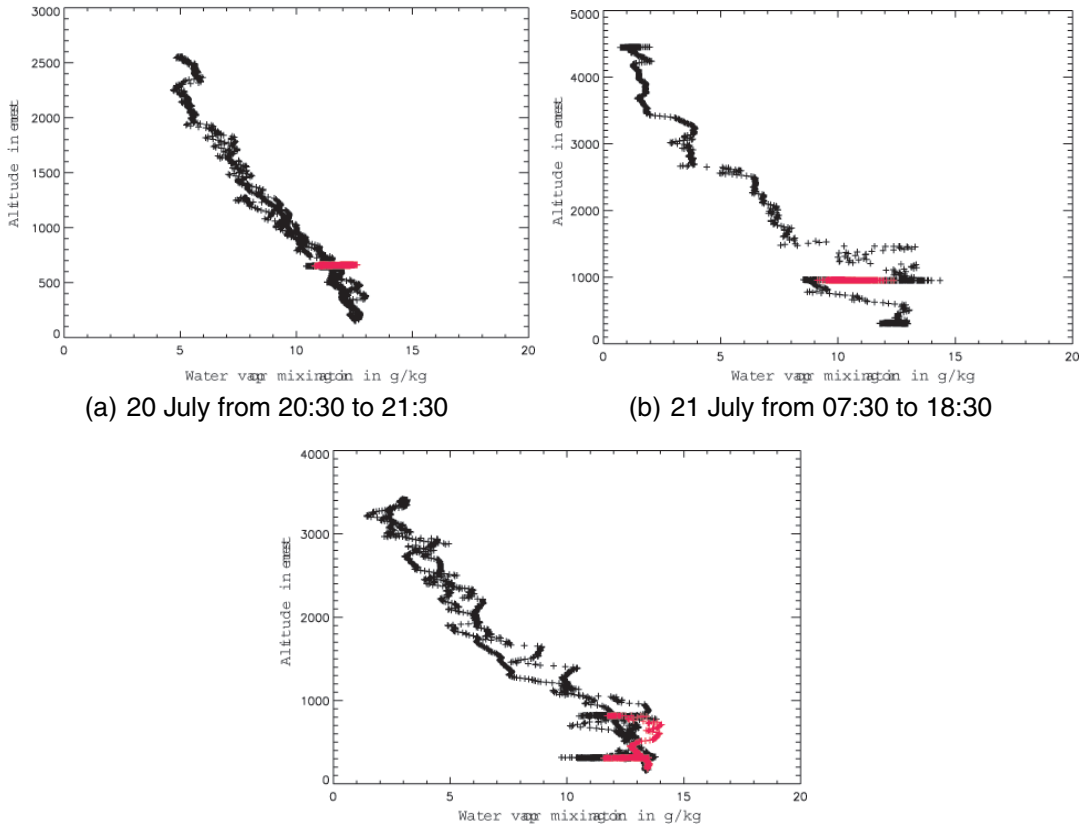

(a) 20 July from 20:30 to 21:30

(b) 21 July from 07:30 to 18:30

(c) 22 July from 17:00 to 18:00

Fig. 7. Vertical water vapour profiles measured by the P3 close to the Lagrangian matches on 20, 21 and 22 July. Measurements made in the Lagrangian matches are coloured in red.

ACPD

8, 7509–7554, 2008

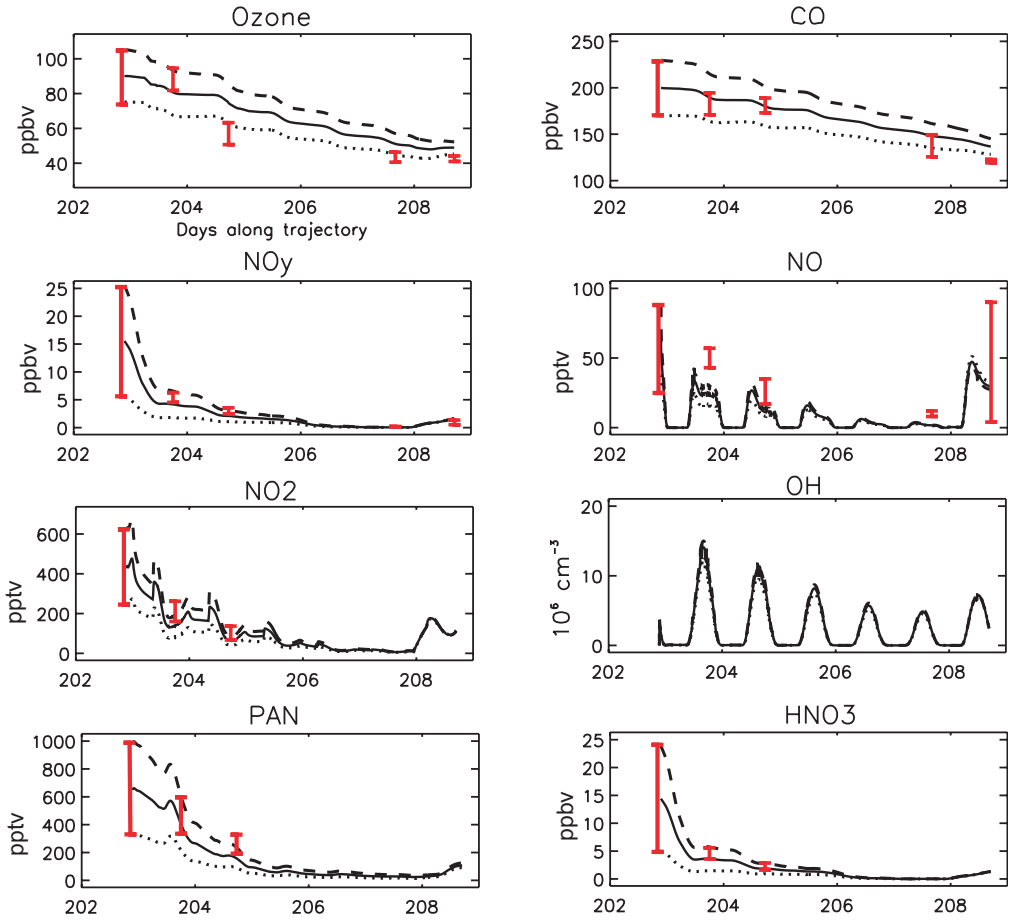

Fig. 8. Modelled concentrations for runs including chemical, deposition and mixing processes using mean ± std concentrations (same as Fig. 4).

ACPD
8, 7509–7554, 2008

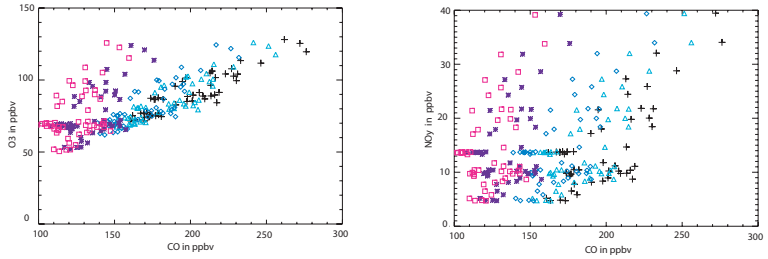

(a) Chemistry only simulation.

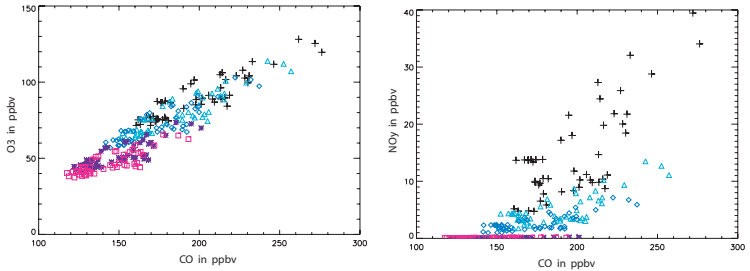

(b) Simulation including deposition.

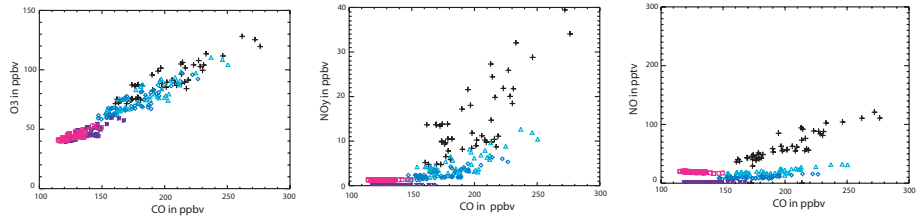

(c) Simulation including deposition and mixing.

Fig. 9. Simulated concentrations of O_3, NO_y and NO versus simulated CO concentrations in the 5 Lagrangian samplings. Black crosses represent measurement in the 20 July Lagrangian match and green triangles, blue diamonds, pink squares and violet stars show the simulated concentrations on 21, 22, 25 and 26 Lagrangian samplings, respectively.

ACPD
8, 7509–7554, 2008

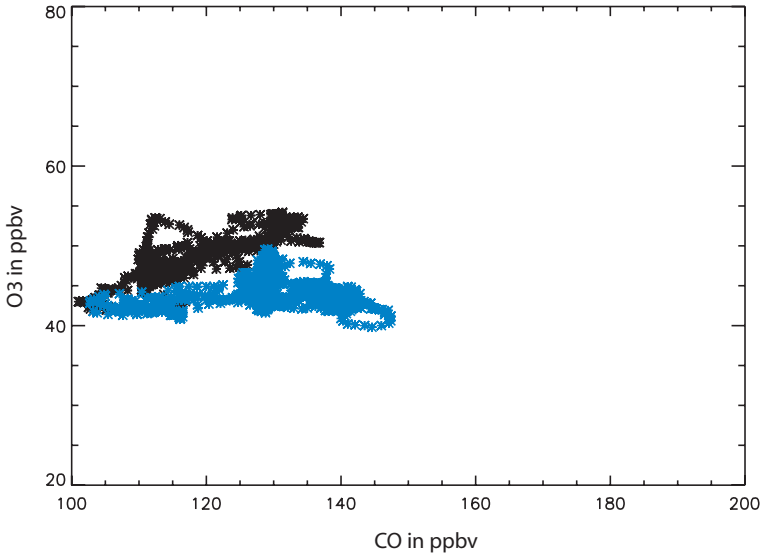

Fig. 10. Measured O_3 concentrations versus CO concentrations in the 25 July Lagrangian match from 15:54 to 16:09 (blue crosses, part 1) and from 16:09 to 16:21 (black crosses, part 2).

ACPD
8, 7509–7554, 2008